Supporting information:

Ionic aggregation-induced emission: bulky hydrophobic counterions light up dyes in polymeric nanoparticles

*Ilya O. Aparin, Nina Melnychuk, and Andrey S. Klymchenko**

Table of contents

Experimental section

Methods and materials: All the reagents were purchased from commercial suppliers: Sigma-Aldrich, Alfa Aesar or Tokyo Chemical Industry and used as received. Sodium tetraphenylborate (TPB), sodium tetrakis[3,5-bis(1,1,1,3,3,3-hexafluoro-2-methoxy-2-propyl)phenyl]borate trihydrate (F12-TPB) were purchased from Sigma-Aldrich. Potassium tetrakis(pentafluorophenyl)borate (F5-TPB) was purchased from Alfa Aesar. Poly(methyl methacrylate-co-methacrylic acid (PMMA-MA) copolymer (CAS number: 25086-15-1, 1.6% methacrylic acid, $M_n \approx 15000$, and $M_w \approx 34000$) was purchased from Sigma Aldrich and used as it is. MilliQ-water (Millipore) was used in all experiments. All acetonitrile stock solutions of the dyes were centrifuged for at 14000 RPM for 15 min prior to use, MilliQ-water and 20 mM phosphate buffer were filtered through a PES Millipore syringe filter directly before NPs preparation.

NMR spectra of the synthesized compounds were recorded at 20°C on a Bruker Avance III 400 MHz spectrometer. Mass spectra were obtained using an Agilent Q-TOF 6520 mass spectrometer. Absorption spectra were recorded on Varian Cary 5000 UV-Vis-NIR spectrophotometer (Agilent). Fluorescence steady state spectra and anisotropy spectra were recorded on an Edinburgh FS5 spectrofluorometer. Fluorescence quantum yields of the dyes and NPs solutions were calculated using Nile Red in methanol as a reference (QY = 38%).[84] Absorption and fluorescence spectra were recorded for three separately prepared samples for QY determination. Averaged values for fluorescence QY are given. DLS measurements of the nanoparticles size by volume were performed on Zetasizer Nano ZSP (Malvern Instruments S.A.). Each DLS measurement was repeated three times for three separately prepared NPs samples. The average values of the size distribution per volume were presented.

Nanoparticle preparation: NPs of pure dye/counterion pairs were performed according to the protocol developed previously by us.[57] In brief, 10 μL of 1 mM **EtSP18**, **PhSP18** or **CzSP18** iodides solutions in acetonitrile was precipitated under vigorous stirring to 1.9 mL of water. Then, 10 equivalents of the corresponding salt were added as 1 mM water solution (100 μL) under stirring. The resultant NPs were directly used for measurements without dilution.

Dye-loaded polymeric PMMA-MA NPs with different loading of the dyes were obtained by nanoprecipitation.[14] Stock solutions of PMMA-MA (1 mg/mL) in acetonitrile were prepared containing 20 mM, 50 mM, 100 mM, 200 mM, 300 mM, 400 mM and 500 mM of **EtSP18**, **PhSP18** and **CzSP18** per PMMA-MA with $\mathbf{I^-}$, $\mathbf{ClO_4^-}$, $\mathbf{PF_6^-}$, **F5-TPB**, **F12-TPB** counterions. The stock solutions (50 μL) were quickly precipitated using a micropipette to 20 mM phosphate buffer (450 μL) with pH 7.4 at 21°C under shaking (Thermomixer comfort, Eppendorf, 1100 rpm). Obtained nanoparticles solutions were diluted five-fold with 20 mM phosphate buffer. These solutions were further used for DLS and spectroscopy measurements.

Single-particle fluorescence measurements: For single-particle fluorescence microscopy measurements, the NPs were immobilized on the glass surface (LabTek 8-well plate), which was washed with 1 M KOH aqueous solution and then treated with polyethylenimine (PEI), as described before.[59] The solutions of NPs were diluted 1000 times from initial preparation, and 250 μl of the diluted NPs were deposited on the PEI-covered glass for 30 min. QD605 (10 pM) were immobilized onto the glass surfaces using the same protocol. Then, the chamber was rinsed 3 times with 20 mM phosphate buffer (pH 7.4) and measurements were performed

with a layer of the same buffer (300 µL) above the surface. Single-particle measurements were performed in the wide-field epi-fluorescence mode using a Nikon Ti-E inverted microscope with a 100× objective (Apo TIRF, oil, NA 1.49, Nikon). The excitation was provided by light-emitting diodes (SpectraX, Lumencor) at 470 nm. The emission was recorded at >500 nm with a long-pass filter. The power density was 0.51 W cm^{-2} for **EtSP18**/[**F5-TPB**], **PhSP18**/[**F5-TPB**], **CzSP18**/[**F5-TPB**] NPs with 50 mM and 500 mM loading and 2.54 W cm^{-2} for **PhSP18**/[**F5-TPB**] NPs with 5 mM loading and Qdots605. The presented images were an average of the first 5 frames (recorded at a 200 ms integration time), whereas the time-lapse data were recorded for 60 s with the same integration time. The single-particle analysis was performed using Fiji software.

TEM measurements: Carbon-coated copper–rhodium electron microscopy grids with a 300 mesh (Euromedex) were surface-treated with a glow discharge in an amylamine atmosphere (0.45 mbar, 4–5 mA, 22 s) in an Elmo glow discharge system (Cordouan Technologies). Then, 5 µl of the NPs were placed onto the grids and left for 1 min. The grids were treated with a 2% uranyl acetate solution for staining. Measurements were taken on a Philips CM120 transmission electron microscope equipped with a LaB6 filament and operating at 100 kV. Areas of interest of all the NPs were recorded at different magnifications on a Peltier cooled CCD camera (Model 794, Gatan). The image analysis was then performed using Fiji software.

Synthesis of styryl pyridinium dyes

Synthesis of 4-methyl-1-octadecylpyridin-1-ium iodide: 4-Picoline (93 mg, 1 mmol) and octadecyl iodide (420 mg, 1.1 mmol) in acetonitrile (2 mL) were refluxed for 24 h with intensive stirring. Reaction was cooled to RT and concentrated *in vacuo*. Viscous bulk was refluxed in n-heptane (5 mL) with treating to form yellowish solid precipitate which was filtered hot, washed with diethyl ether (3×20 mL) and dried in air to obtain 468 mg (99%) of product as beige powder. Rf 0.28 (DCM/methanol = 95:5, v/v). 1H NMR (400.13 MHz, chloroform-d, δ): 9.22 (d, J = 6.7 Hz, 2H), 7.90 (d, J = 6.4 Hz, 2H), 4.83 (t, J = 7.5 Hz, 1H), 2.66 (s, 3H), 1.99 (m, 2H), 1.36-1.18 (m, 30H), 0.84 (m, 3H); 13C NMR (100.61 MHz, CDCl3, δ): 158.86, 143.94, 128.85, 77.21, 61.23, 31.78, 31.63, 29.57, 29.52, 29.49, 29.25, 29.22, 28.95, 25.89, 22.55, 22.28, 13.98; HRMS (ESI) m/z: $[M\text{-}I]^+$ calcd. for $C_{24}H_{44}N^+$, 346.3468; found 346.3477.

Synthesis of (E)-4-(4-(diethylamino)styryl)-1-octadecylpyridin-1-ium iodide (**EtSP18**)*:* 4-Methyl-1-octadecylpyridin-1-ium iodide (94 mg, 0.2 mmol), 4-diethylaminobenzaldehyde (35 mg, 0.2 mmol), piperidine (1 drop) in absolute ethanol (1 mL) were refluxed in inert atmosphere with stirring for 4 h. Reaction was cooled to RT, crystals were separated by filtration and recrystallized twice from absolute ethanol to obtain 91 mg (72%) as red crystals. Rf 0.25 (DCM/methanol = 95:5, v/v). 1H NMR (400.13 MHz, chloroform-d, δ): 8.76 (d, J = 6.9 Hz, 2H), 7.87 (d, J = 6.9 Hz, 2H), 7.62 (d, J = 15.9 Hz, 1H), 7.53 (d, J = 9.0 Hz, 2H), 6.85 (d, J = 15.8 Hz, 1H), 6.66 (d, J = 9.0 Hz, 2H), 4.53 (t, J = 7.3 Hz, 2H), 3.42 (q, J = 7.0 Hz, 4H), 1.91 (m, 2H), 1.36-1.15 (m, 36H), 0.87 (m, 3H); 13C NMR (100.61 MHz, CDCl3, δ): 154.24, 150.17, 143.12, 142.94, 131.16, 122.56, 121.65, 115.66, 111.49, 77.21, 60.23, 44.59, 31.86, 31.46, 29.64, 29.60, 29.55, 29.46, 29.33, 29.29, 26.02, 22.62, 14.05 12.58; HRMS (ESI) m/z: $[M\text{-}I]^+$ calcd. for $C_{35}H_{57}N_2^+$, 505.4516; found 505.4527.

Synthesis of (E)-4-(4-(diphenylamino)styryl)-1-octadecylpyridin-1-ium iodide (**PhSP18**)*:* 4-Methyl-1-octadecylpyridin-1-ium iodide (94 mg, 0.2 mmol), 4-(dimethylamino)benzaldehyde (55 mg, 0.2 mmol), piperidine (1 drop) in absolute ethanol (1 mL) were refluxed in inert atmosphere with stirring for 8 h. Reaction was cooled to RT, all volatiles were removed *in vacuo*. Solid precipitate was recrystallized sequentially from acetonitrile and absolute ethanol to obtain 123 mg (85%) as red crystals. Rf 0.30 (DCM/methanol = 95:5, v/v). 1H NMR (400.13 MHz, chloroform-d, δ): 9.05 (d, J = 6.8 Hz, 2H), 8.12 (d, J = 6.9 Hz, 2H), 7.81 (d, J = 16.1 Hz, 1H), 7.63 (d, J = 8.8 Hz, 2H), 7.46-7.41 (m, 4H), 7.28-7.22 (m, 6H), 7.15-7.11 (m, 3H), 4.79 (t, J = 7.3 Hz, 2H), 2.09 (m, 3H), 1.50-1.33 (m, 30H), 1.00 (m, 3H); 13C NMR (100.61 MHz, CDCl3, δ): 153.83, 150.65, 146.33, 143.53, 142.06, 129.92, 129.56, 127.03, 125.76, 124.58, 123.42, 120.78, 118.87, 77.21, 60.68, 50.65, 31.84, 31.51, 29.63, 29.58, 29.56, 29.45, 29.31, 29.28, 29.01, 26.01, 22.61, 14.04; HRMS (ESI) m/z: $[M-I]^+$ calcd. for $C_{43}H_{57}N_2^+$, 601.4516; found 601.4526.

Synthesis of (E)-4-(4-(9H-carbazol-9-yl)styryl)-1-octadecylpyridin-1-ium iodide (**CzSP18**): 4-Methyl-1-octadecylpyridin-1-ium iodide (94 mg, 0.2 mmol), 9-(4-formylphenyl)carbazole (54 mg, 0.2 mmol), piperidine (1 drop) in absolute ethanol (1 mL) were refluxed in inert atmosphere with stirring for 24 h. Reaction was cooled to RT, all volatiles were removed *in vacuo*. Solid precipitate was recrystallized sequentially from acetonitrile and absolute ethanol to obtain 76 mg (52%) as yellow crystals. Rf 0.21 (DCM/methanol = 95:5, v/v). 1H NMR (400.13 MHz, chloroform-d, δ): 8.87 (d, J = 6.5 Hz, 2H), 8.01 (d, J = 6.7 Hz, 2H), 7.94 (d, J = 7.7 Hz, 2H), 7.72 (m, 3H), 7.43 (d, J = 8.4 Hz, 2H), 7.28-7.10 (m, 8H), 4.56 (t, J = 7.3 Hz, 2H), 1.81 (m, 2H), 1.20-1.00 (m, 30H), 0.69 (m, 3H); 13C NMR (100.61 MHz, CDCl3, δ): 153.37, 143.97, 141.10, 140.11, 139.99, 133.08, 130.03, 126.92, 126.15, 124.42, 123.73, 122.54, 120.53, 120.39, 109.75, 77.21, 61.12, 31.87, 31.61, 29.65, 29.61, 29.57, 29.48, 29.34, 29.30, 29.04, 26.05, 22.63, 14.06; HRMS (ESI) m/z: $[M-I]^+$ calcd. for $C_{43}H_{55}N_2^+$, 599.4360; found 599.4367.

General procedure for the ion-exchange of the dyes: Prepared **EtSP18**, **PhSP18** and **CzSP18** in iodide form (10 μmmol) were dissolved in DCM (1 mL) and 10 equivalents of inorganic salt: $NaClO_4$ or KPF_6, or 3 equivalents of potassium tetrakis (pentafluorophenyl)borate ethyl etherate **[F5-TPB]** or sodium tetrakis[3,5-bis-(1,1,1,3,3,3-hexafluoro-2-methoxy-2-propyl)phenyl]borate **[F12-TPB]** in water (1 mL) were added. Two-phase solutions were shaken for 30 min at RT, and then TLC showed complete conversion to individually pure spots. DCM layer was separated, the water phase was extracted additionally with DCM, if need. Combined DCM solutions were passed through a cotton filter and evaporated *in vacuo* to dryness. Solid residue was dissolved in DCM (200 μL) and passed through a silica gel column, eluting with pure DCM or DCM/ethyl acetate (9:1, v/v) mixture. Fractions were concentrated *in vacuo* to obtain the final dye/counterion pairs with quantitative yield and characterized with TLC (Figure S35).

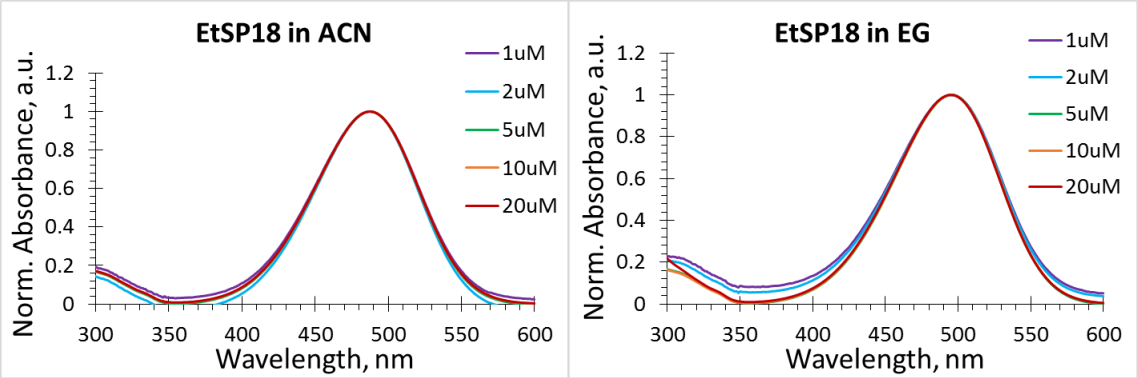

Figure S1. Normalized absorption spectra of **EtSP18 [ClO_4^-]** in acetonitrile and ethylene glycol of different concentrations.

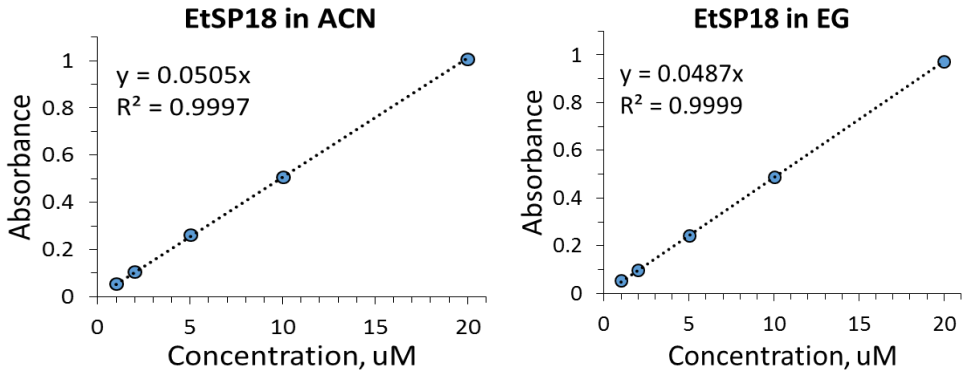

Figure S2. Relationship between **EtSP18 [ClO_4^-]** concentration and absorption maxima value.

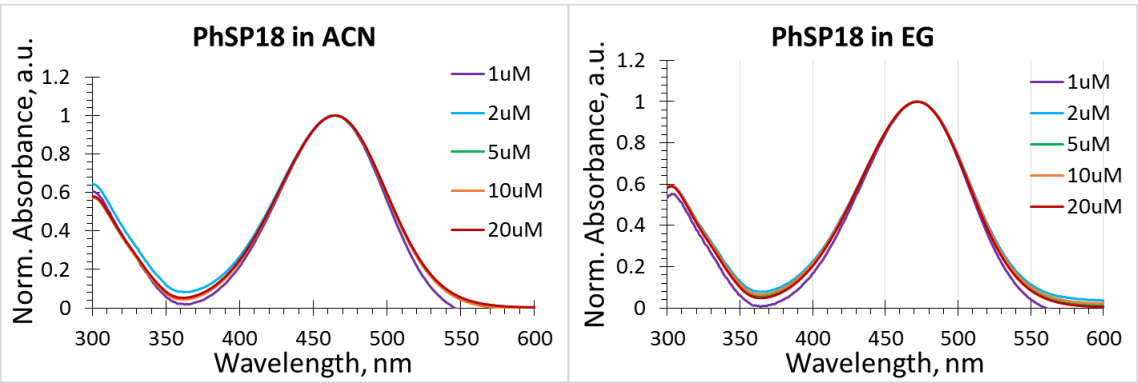

Figure S3. Normalized absorption spectra of **PhSP18 [ClO_4^-]** in acetonitrile and ethylene glycol of different concentrations.

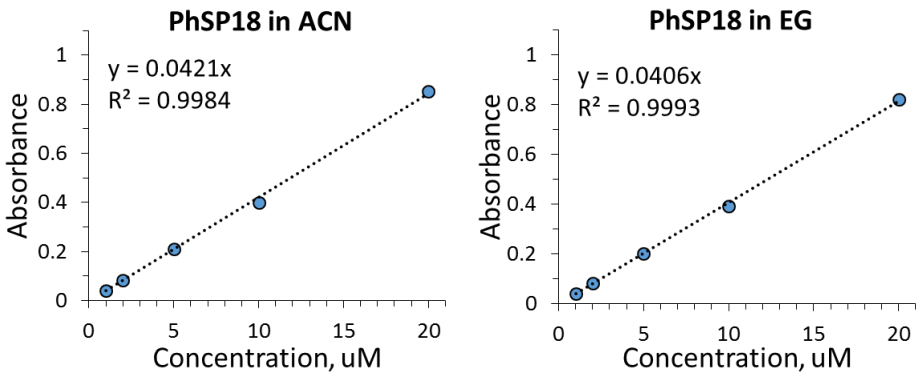

Figure S4. Relationship between **PhSP18 [ClO_4^-]** concentration and absorption maxima value.

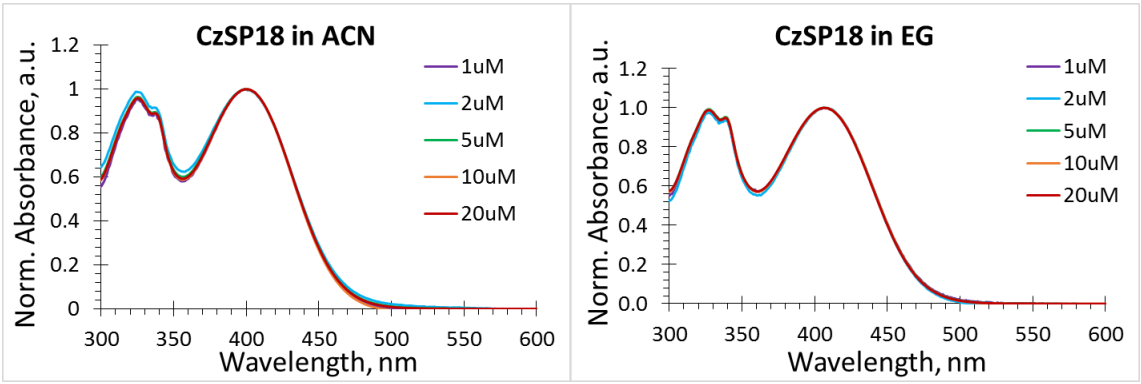

Figure S5. Normalized absorption spectra of **CzSP18 [ClO_4^-]** in acetonitrile and ethylene glycol of different concentrations.

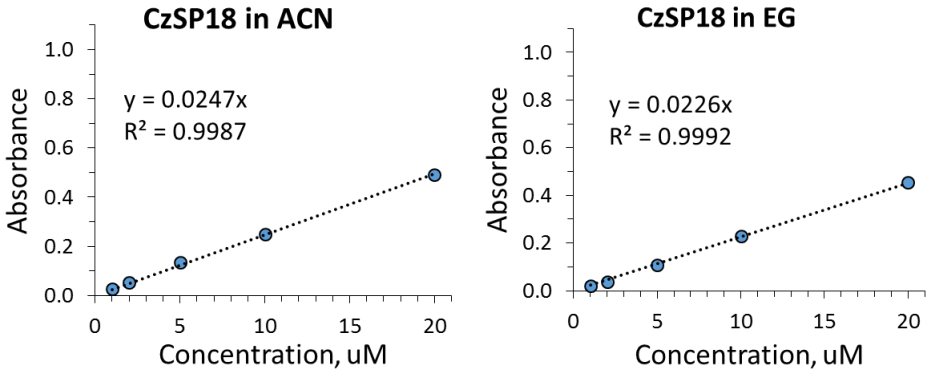

Figure S6. Relationship between **CzSP18 [ClO_4^-]** concentration and absorption maxima value.

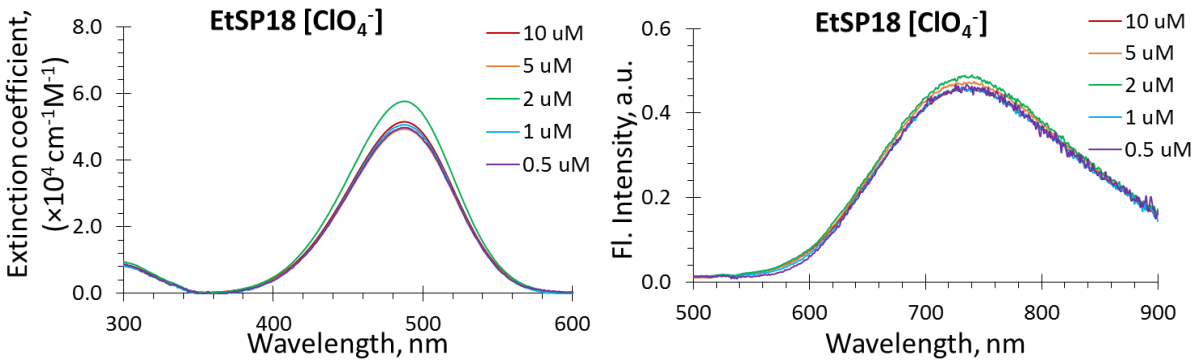

Figure S7. Absorption and fluorescence spectra of **EtSP18 [ClO$_4^-$]** in acetonitrile of different concentrations. Fluorescence spectra were divided by absorbance values at the excitation wavelength.

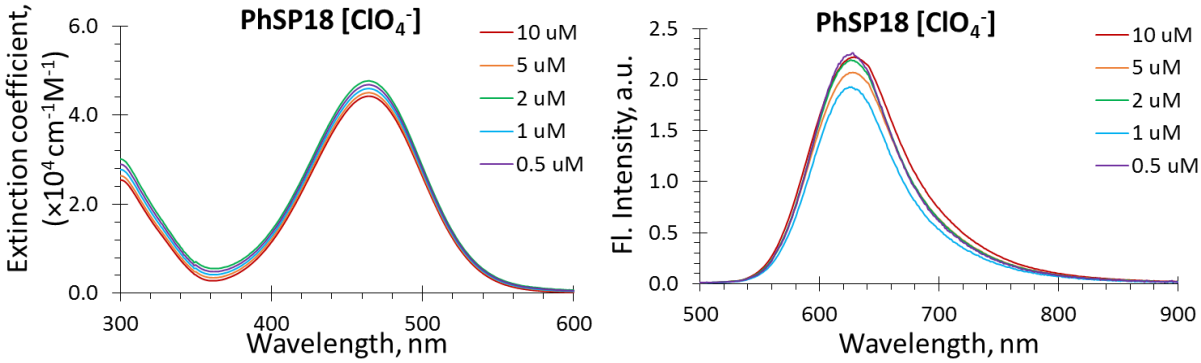

Figure S8. Absorption and fluorescence spectra of **PhSP18 [ClO$_4^-$]** in acetonitrile of different concentrations. Fluorescence spectra were divided by absorbance values at the excitation wavelength.

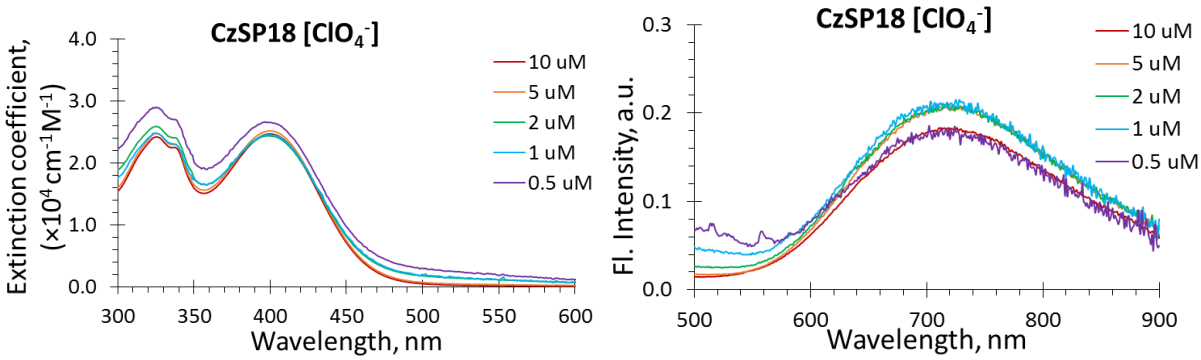

Figure S9. Absorption and fluorescence spectra of **CzSP18 [ClO$_4^-$]** in acetonitrile of different concentrations. Fluorescence spectra were divided by absorbance values at the excitation wavelength.

Table S1. Average size by volume and polydispersity (PDI) of precipitated dye^+/$counterion^-$ NPs by dynamic light scattering (DLS).

Name	Counterion	Average size, nm	PDI
EtSP18	[I^-]	36.8±10.9	0.389
	[ClO_4^-]	58.5±12.5	0.360
	[PF_6^-]	57.9±38.1	0.451
	[TPB]	52.6±32.7	0.271
	[F5-TPB]	55.2±20.7	0.171
	[F12-TPB]	62.8±33.5	0.209
PhSP18	[I^-]	42.6±26.1	0.505
	[ClO_4^-]	54.6±37.2	0.424
	[PF_6^-]	51.8±12.1	0.268
	[TPB]	60.4±10.6	0.126
	[F5-TPB]	54.3±6.5	0.197
	[F12-TPB]	72.7±26.5	0.163
CzSP18	[I^-]	59.0±27.2	0.291
	[ClO_4^-]	78.2±45.3	0.464
	[PF_6^-]	88.4±38.8	0.362
	[TPB]	79.7±32.6	0.238
	[F5-TPB]	62.3±10.1	0.130
	[F12-TPB]	82.1±30.6	0.212

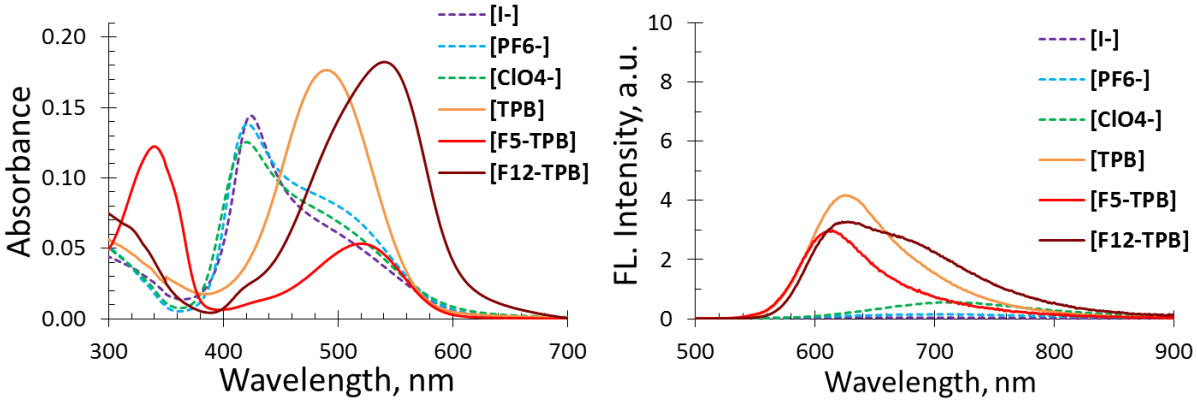

Figure S10. Absorption (left) and fluorescence (right) spectra of **EtSP18** NPs with different counterions in water. Fluorescence spectra were divided by absorbance values at the excitation wavelength. (λ_{exc} = 460±2 nm, concentration of **EtSP18** is 5 μM).

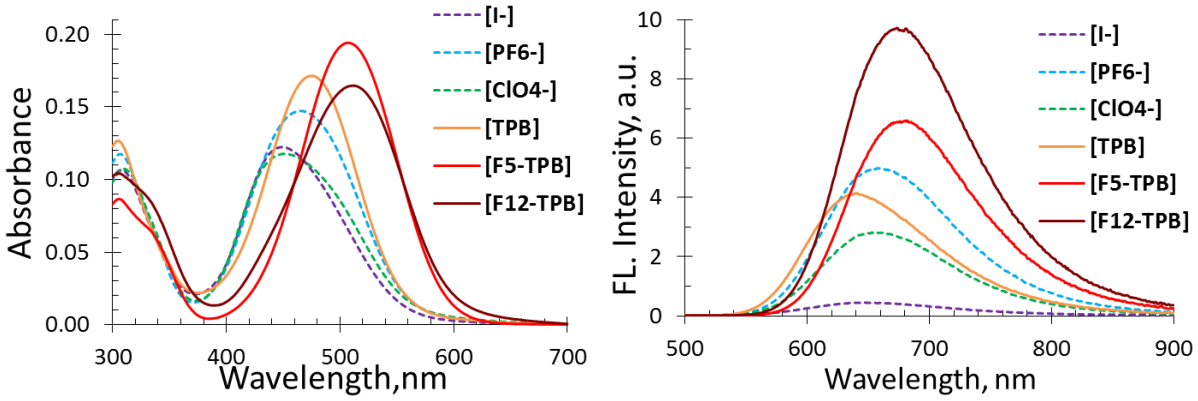

Figure S11. Absorption (left) and fluorescence (right) spectra of **PhSP18** NPs with different counterions in water. Fluorescence spectra were divided by absorbance values at the excitation wavelength. (λ_{exc} = 460±2 nm, concentration of **PhSP18** is 5 μM)

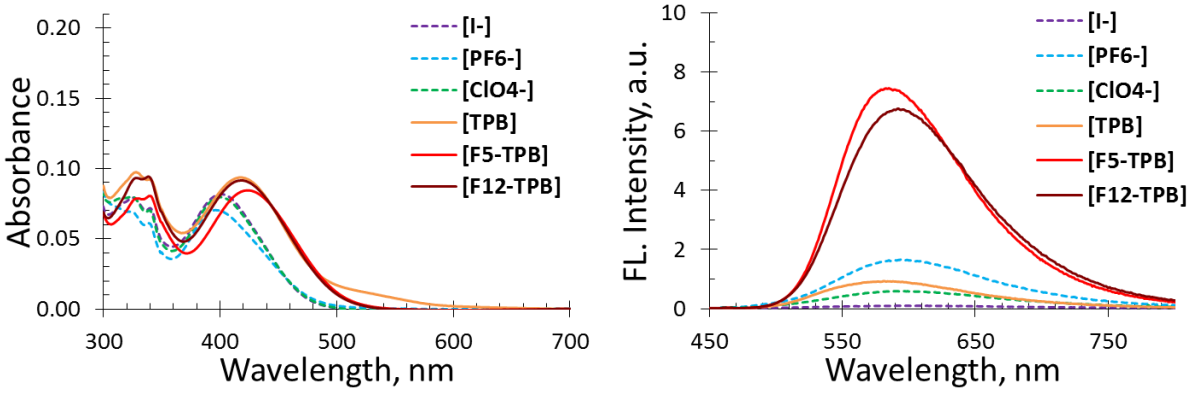

Figure S12. Absorption (left) and fluorescence (right) spectra of **CzSP18** NPs with different counterions in water. Fluorescence spectra were divided by absorbance values at the excitation wavelength. (λ_{exc} = 400±2 nm, concentration of **CzSP18** is 5 μM)

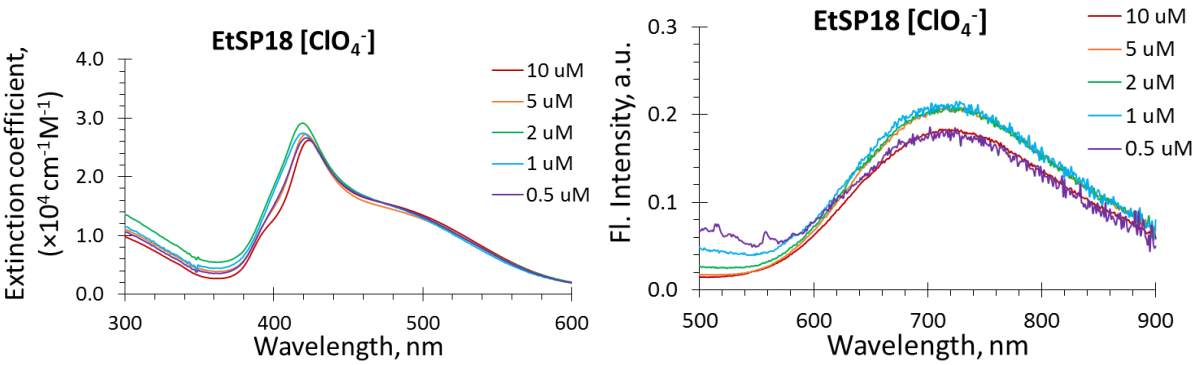

Figure S13. Absorption and fluorescence spectra of **EtSP18 [ClO_4^-]** NPs in aqueous solution of different concentrations. Fluorescence spectra were divided by absorbance values at the excitation wavelength.

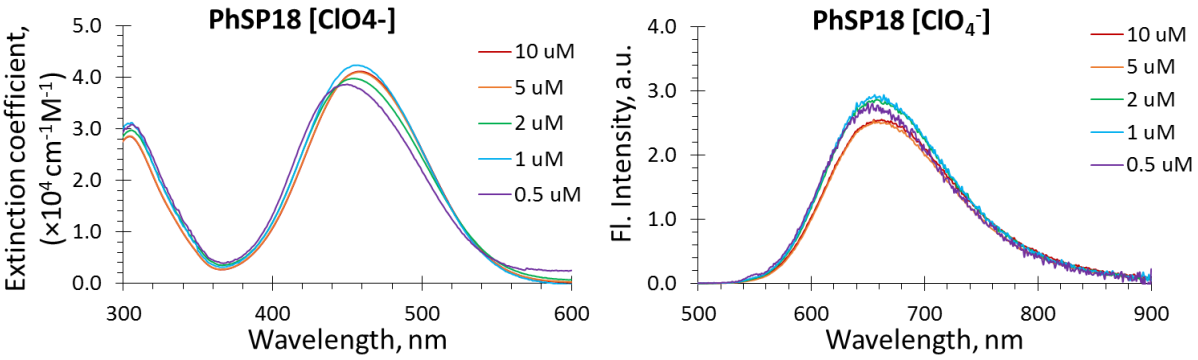

Figure S14. Absorption and fluorescence spectra of **PhSP18 [ClO_4^-]** NPs in aqueous solution of different concentrations. Fluorescence spectra were divided by absorbance values at the excitation wavelength.

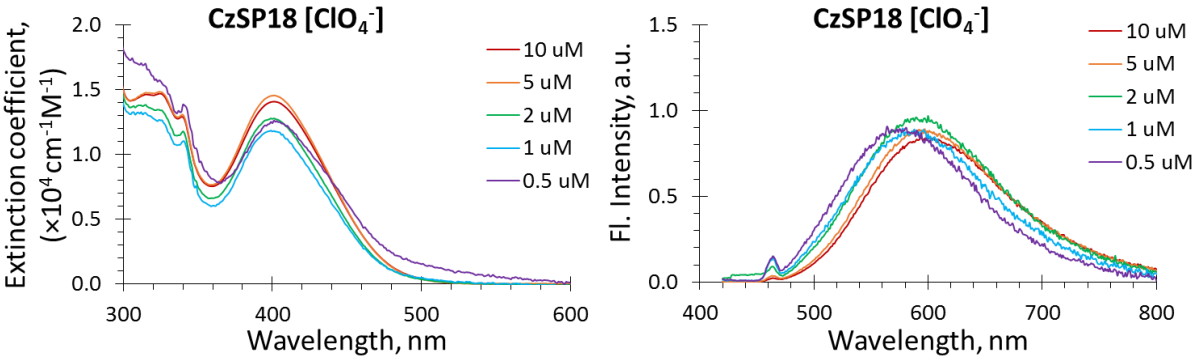

Figure S15. Absorption and fluorescence spectra of **CzSP18 [ClO_4^-]** NPs in aqueous solution of different concentrations. Fluorescence spectra were divided by absorbance values at the excitation wavelength.

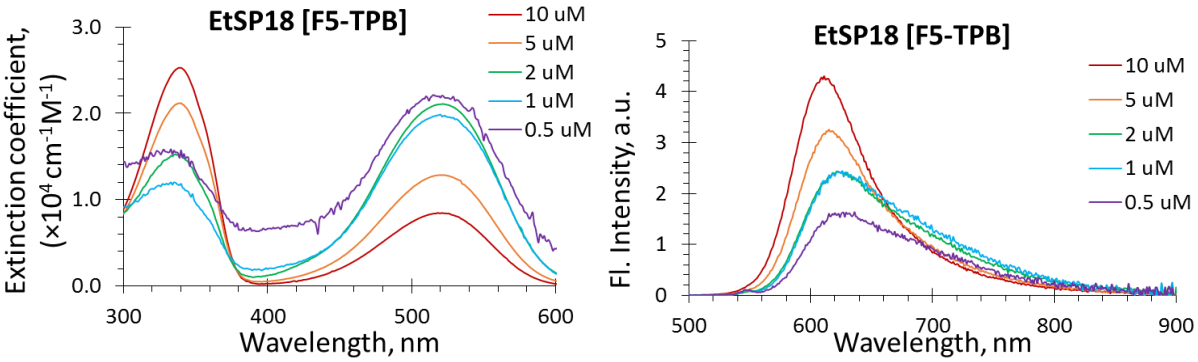

Figure S16. Absorption and fluorescence spectra of **EtSP18 [F5-TPB]** NPs in aqueous solution of different concentrations. Fluorescence spectra were divided by absorbance values at the excitation wavelength.

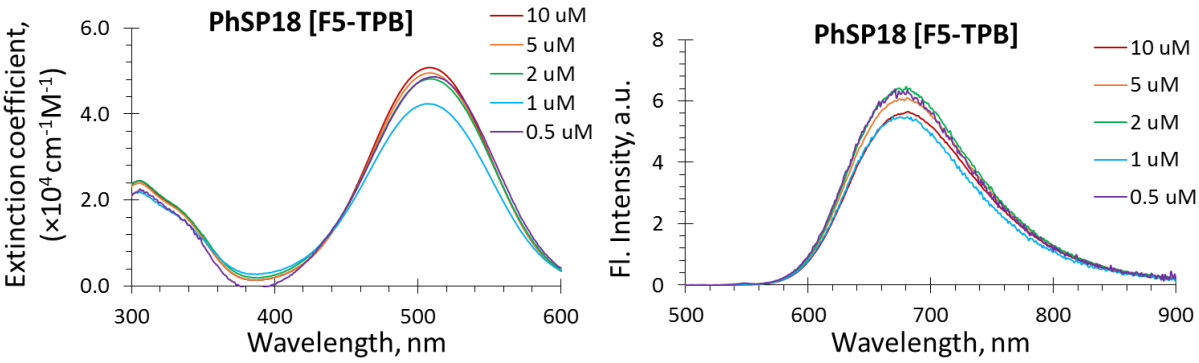

Figure S17. Absorption and fluorescence spectra of **PhSP18 [F5-TPB]** NPs in aqueous solution of different concentrations. Fluorescence spectra were divided by absorbance values at the excitation wavelength.

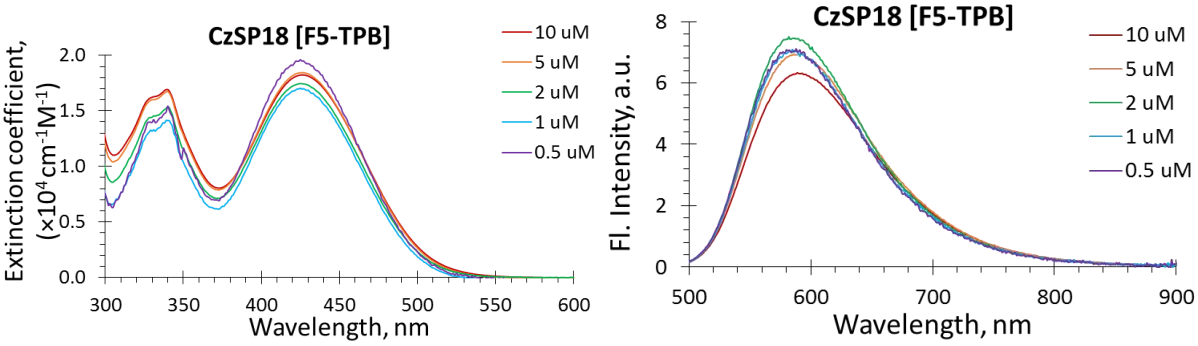

Figure S18. Absorption and fluorescence spectra of **CzSP18 [F5-TPB]** NPs in aqueous solution of different concentrations. Fluorescence spectra were divided by absorbance values at the excitation wavelength.

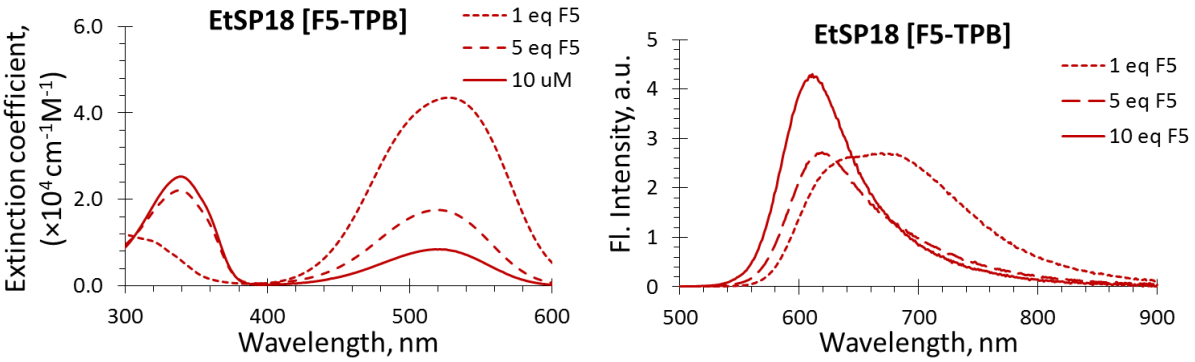

Figure S19. Absorbance and fluorescence spectra of 5 uM **EtSP18** in aqueous solution with different molar ratio of **[F5-TPB]**. Fluorescence spectra were divided by absorbance values at the excitation wavelength.

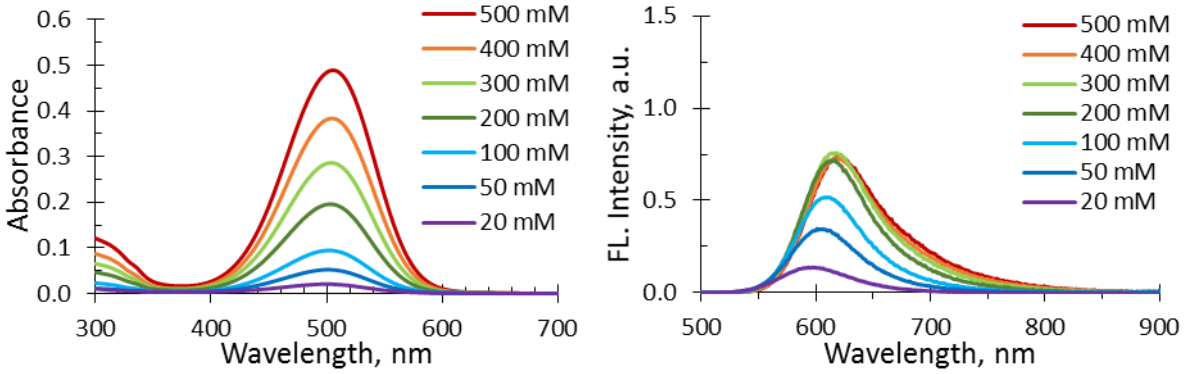

Figure S20. Absorption (left) and fluorescence (right) spectra of PMMA-MA NPs loaded with **EtSP18/[F5-TPB]** of different concentrations in 20 mM phosphate buffer (pH 7.4).

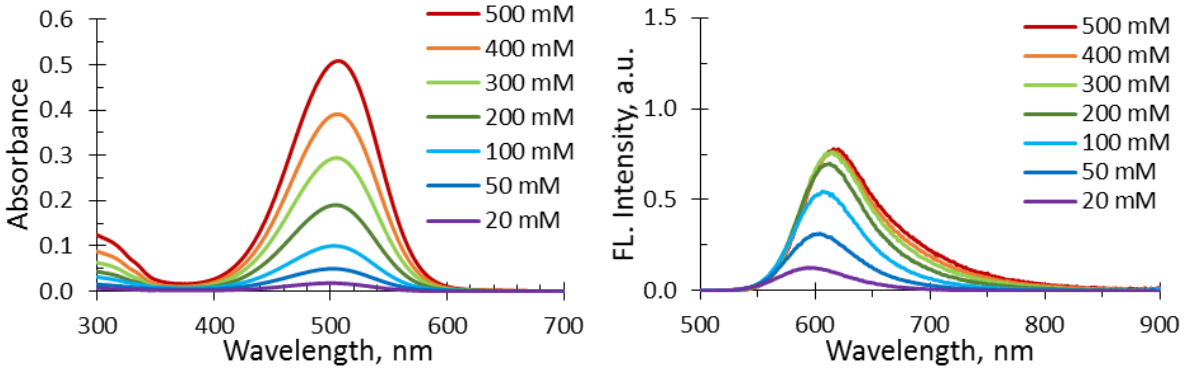

Figure S21. Absorption (left) and fluorescence (right) spectra of PMMA-MA NPs loaded with **EtSP18/[F12-TPB]** of different concentrations in 20 mM phosphate buffer (pH 7.4).

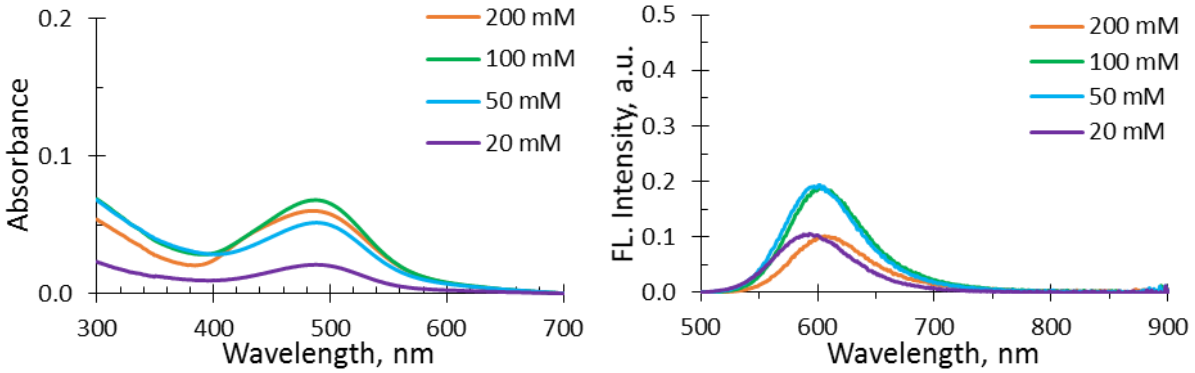

Figure S22. Absorption (left) and fluorescence (right) spectra of PMMA-MA NPs and aggregates loaded with **EtSP18/[I^-]** of different concentrations in 20 mM phosphate buffer (pH 7.4).

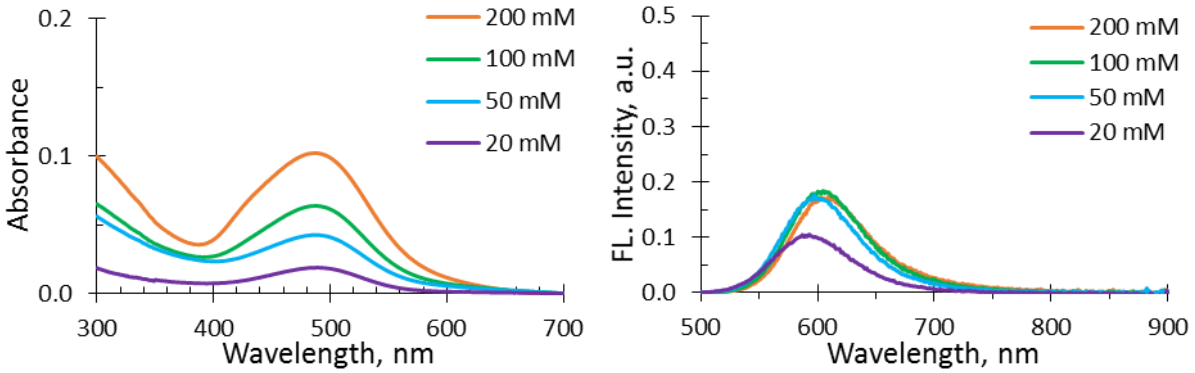

Figure S23. Absorption (left) and fluorescence (right) spectra of PMMA-MA NPs and aggregates loaded with **EtSP18/[ClO_4^-]** of different concentrations in 20 mM phosphate buffer (pH 7.4).

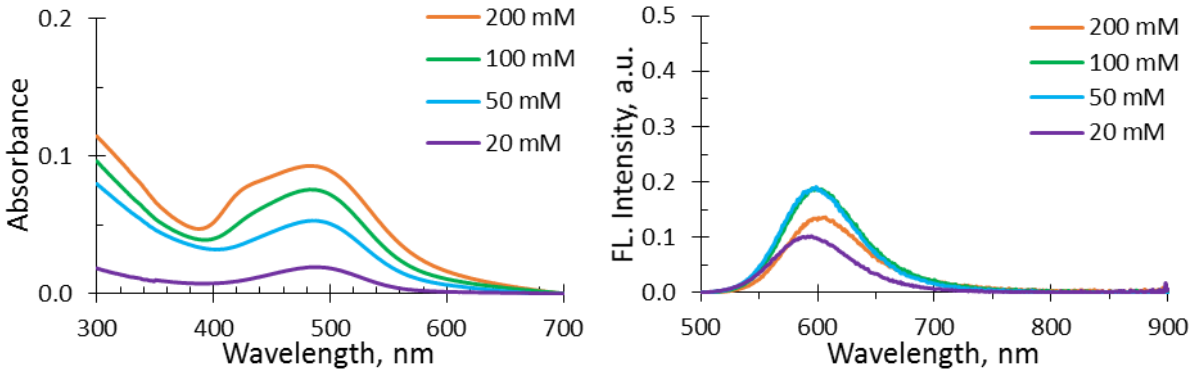

Figure S24. Absorption (left) and fluorescence (right) spectra of PMMA-MA NPs and aggregates loaded with **EtSP18/[PF_6^-]** of different concentrations in 20 mM phosphate buffer (pH 7.4).

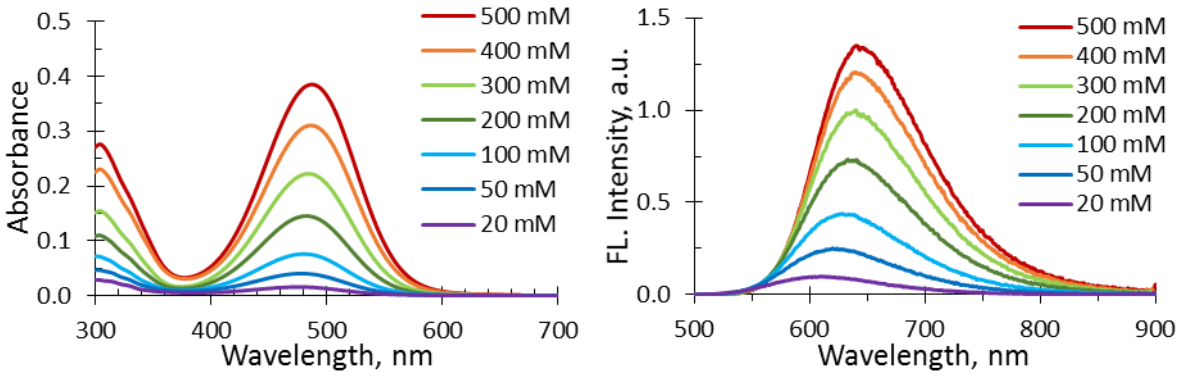

Figure S25. Absorption (left) and fluorescence (right) spectra of PMMA-MA NPs loaded with **PhSP18/[F5-TPB]** of different concentrations in 20 mM phosphate buffer (pH 7.4).

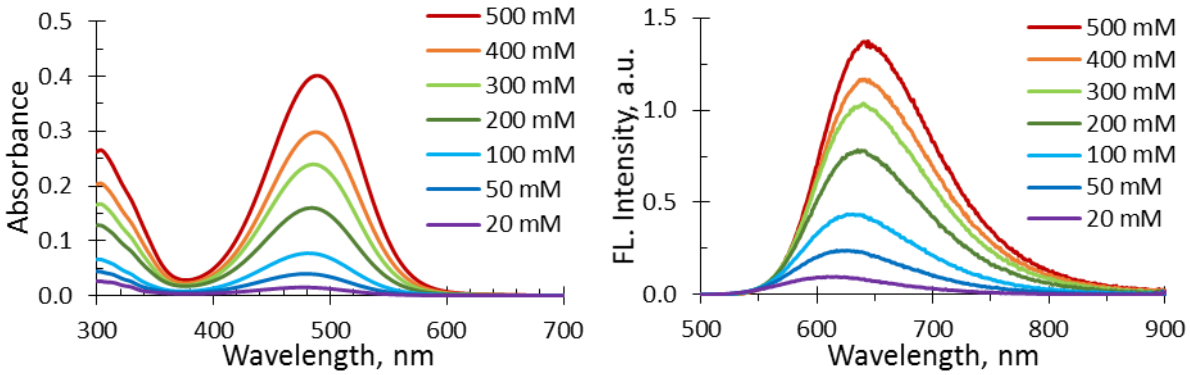

Figure S26. Absorption (left) and fluorescence (right) spectra of PMMA-MA NPs loaded with **PhSP18/[F12-TPB]** of different concentrations in 20 mM phosphate buffer (pH 7.4).

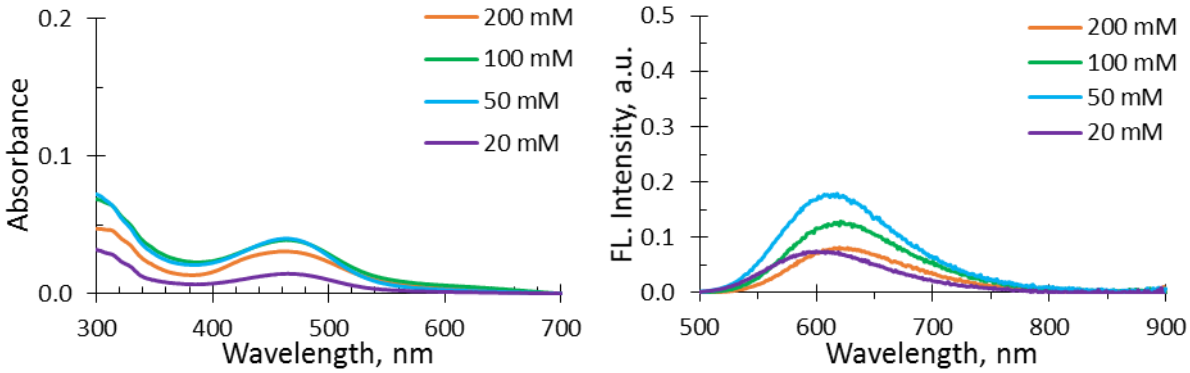

Figure S27. Absorption (left) and fluorescence (right) spectra of PMMA-MA NPs loaded with **PhSP18/[I^-]** of different concentrations in 20 mM phosphate buffer (pH 7.4).

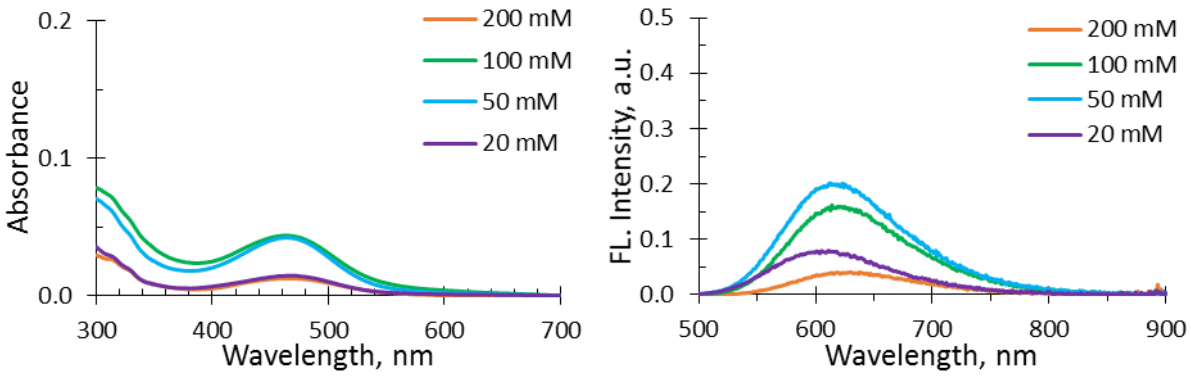

Figure S28. Absorption (left) and fluorescence (right) spectra of PMMA-MA NPs loaded with **PhSP18/[ClO_4^-]** of different concentrations in 20 mM phosphate buffer (pH 7.4).

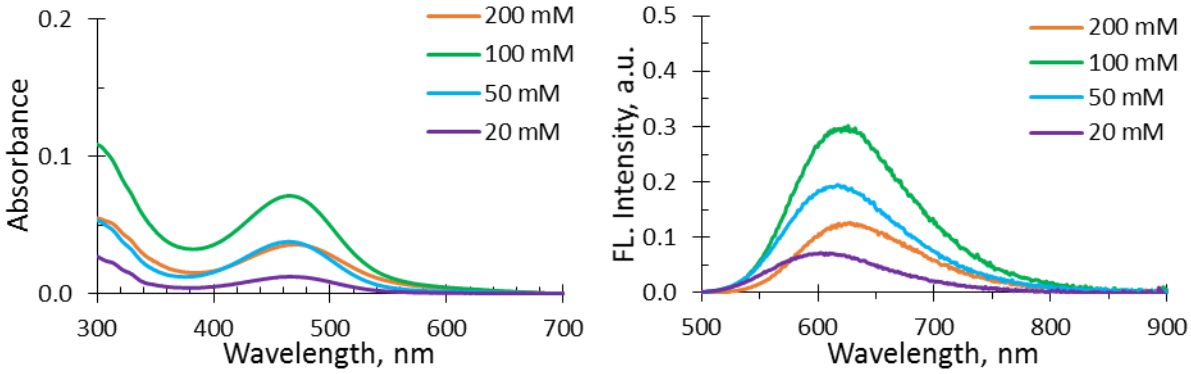

Figure S29. Absorption (left) and fluorescence (right) spectra of PMMA-MA NPs loaded with **PhSP18/[PF_6^-]** of different concentrations in 20 mM phosphate buffer (pH 7.4).

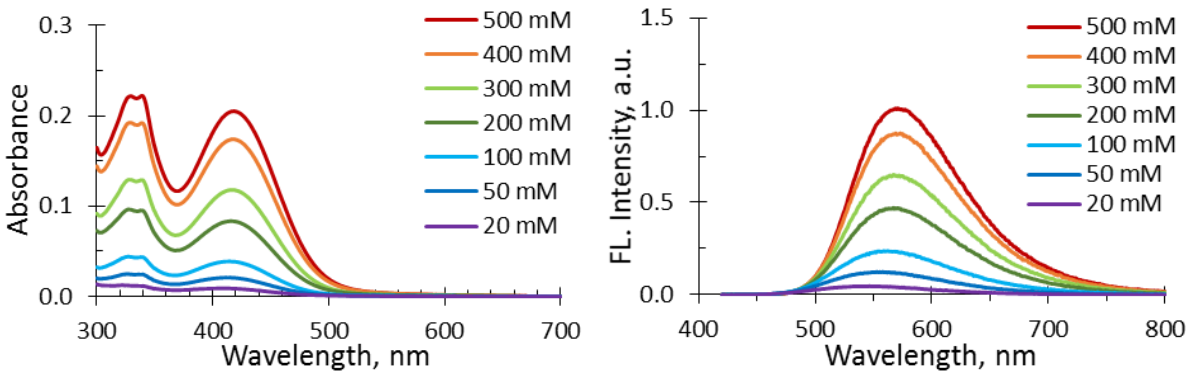

Figure S30. Absorption (left) and fluorescence (right) spectra of PMMA-MA NPs loaded with **CzSP18/[F5-TPB]** of different concentrations in 20 mM phosphate buffer (pH 7.4).

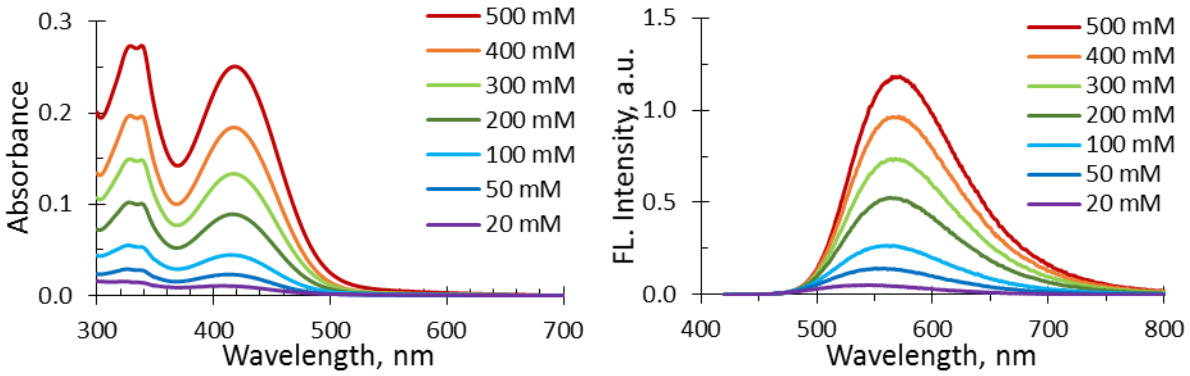

Figure S31. Absorption (left) and fluorescence (right) spectra of PMMA-MA NPs loaded with **CzSP18/[F12-TPB]** of different concentrations in 20 mM phosphate buffer (pH 7.4).

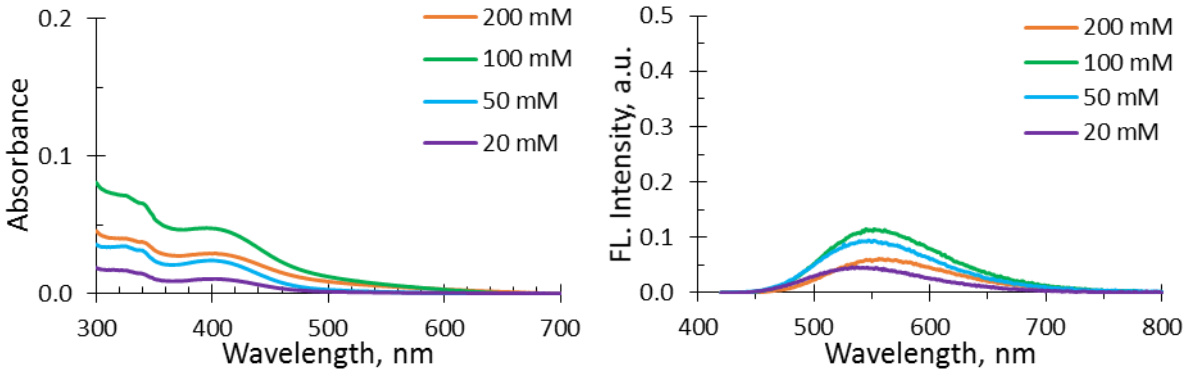

Figure S32. Absorption (left) and fluorescence (right) spectra of PMMA-MA NPs loaded with **CzSP18/[I^-]** of different concentrations in 20 mM phosphate buffer (pH 7.4).

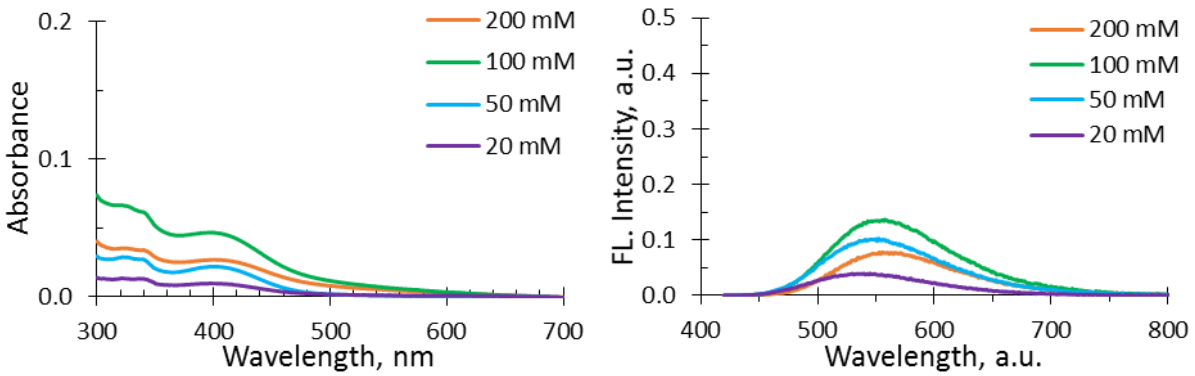

Figure S33. Absorption (left) and fluorescence (right) spectra of PMMA-MA NPs loaded with **CzSP18/[ClO_4^-]** of different concentrations in 20 mM phosphate buffer (pH 7.4).

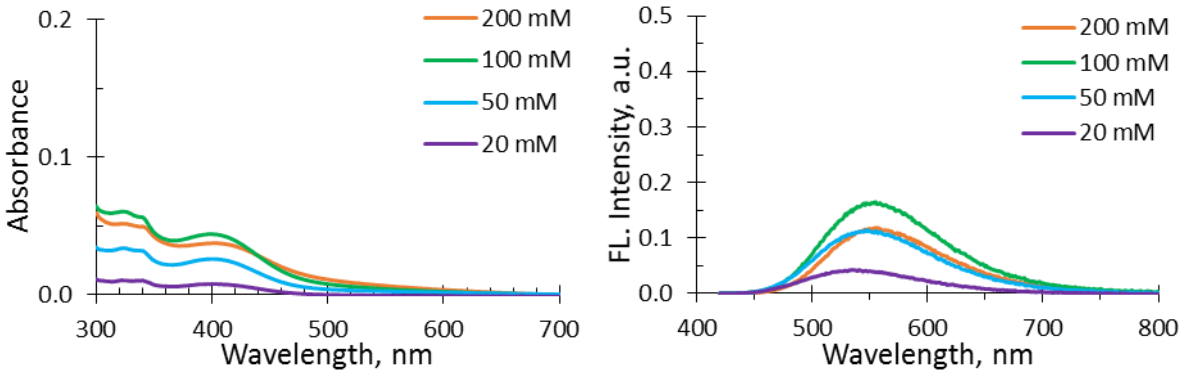

Figure S34. Absorption (left) and fluorescence (right) spectra of PMMA-MA NPs loaded with **CzSP18/[PF_6^-]** of different concentrations in 20 mM phosphate buffer (pH 7.4).

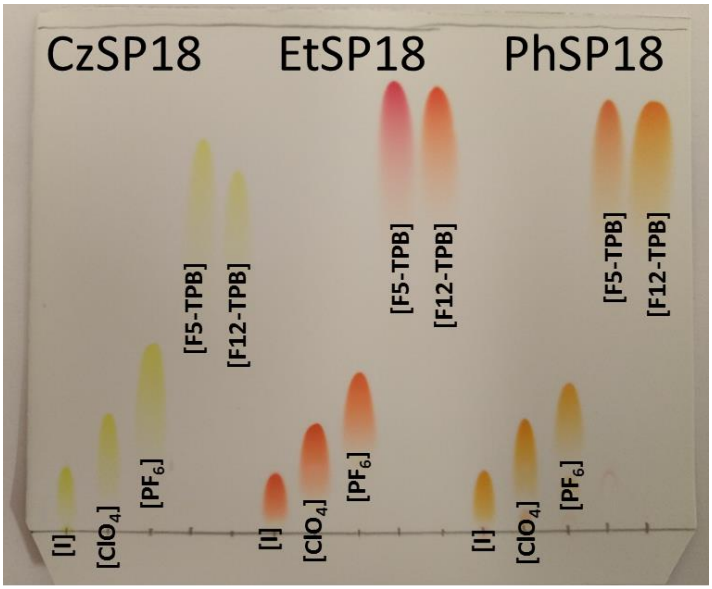

Figure S35. Thin layer chromatography plate of the styryl pyridinium dyes salts with different counterions, eluted with DCM/methanol = 98/2 (v/v).

Table S2. Retention factors (Rf) for the styryl pyridinium dyes with different counterions on TLC plate corresponding to Figure S35.

	CsSP18	**EtSP18**	**PhSP18**
[I]	0.08	0.07	0.08
[ClO4]	0.18	0.17	0.18
[PF6]	0.29	0.27	0.25
[F5-TPB]	0.72	0.83	0.79
[F12-TPB]	0.65	0.81	0.79

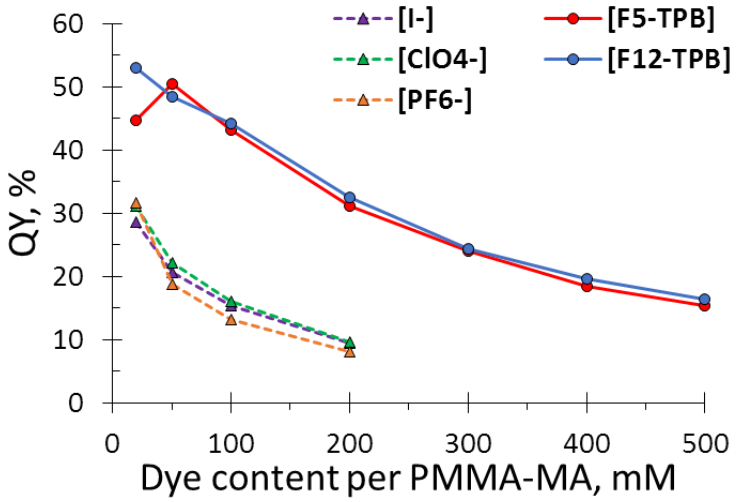

Figure S36. Fluorescence quantum yields of PMMA-MA NPs loaded with **EtSP18** and different counterions vs. dye loading.

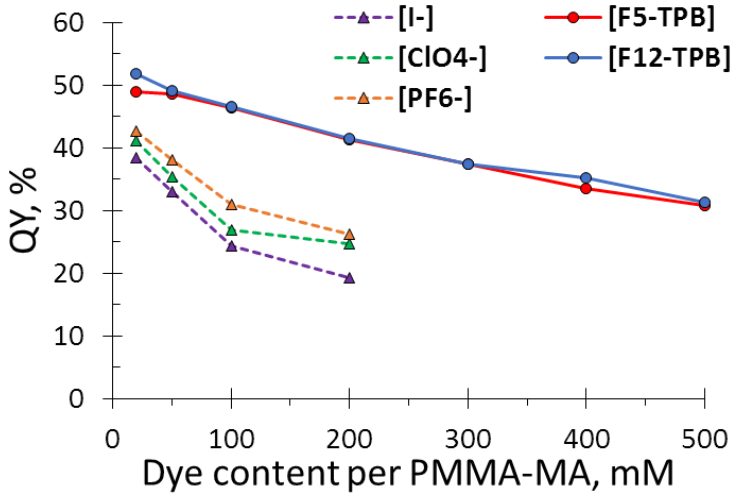

Figure S37. Fluorescence quantum yields of PMMA-MA NPs loaded with **PhSP18** and different counterions vs. dye loading.

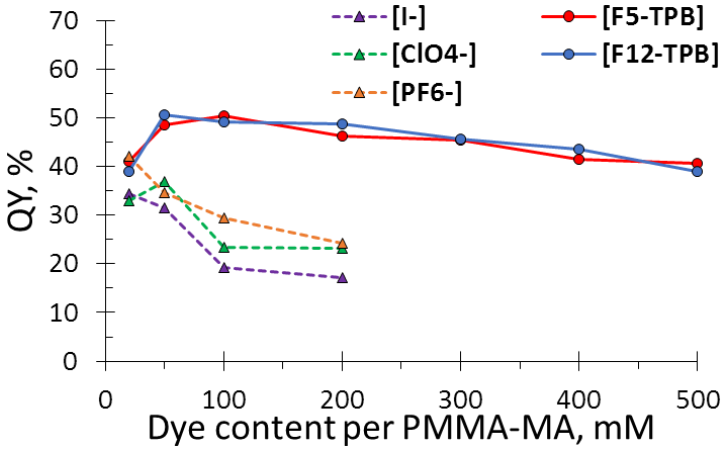

Figure S38. Fluorescence quantum yields of PMMA-MA NPs loaded with **CzSP18** and different counterions vs. dye loading.

^{1}H and ^{13}C NMR spectra of synthesized compounds

4-Methyl-1-octadecylpyridin-1-ium iodide **^{1}H NMR**:

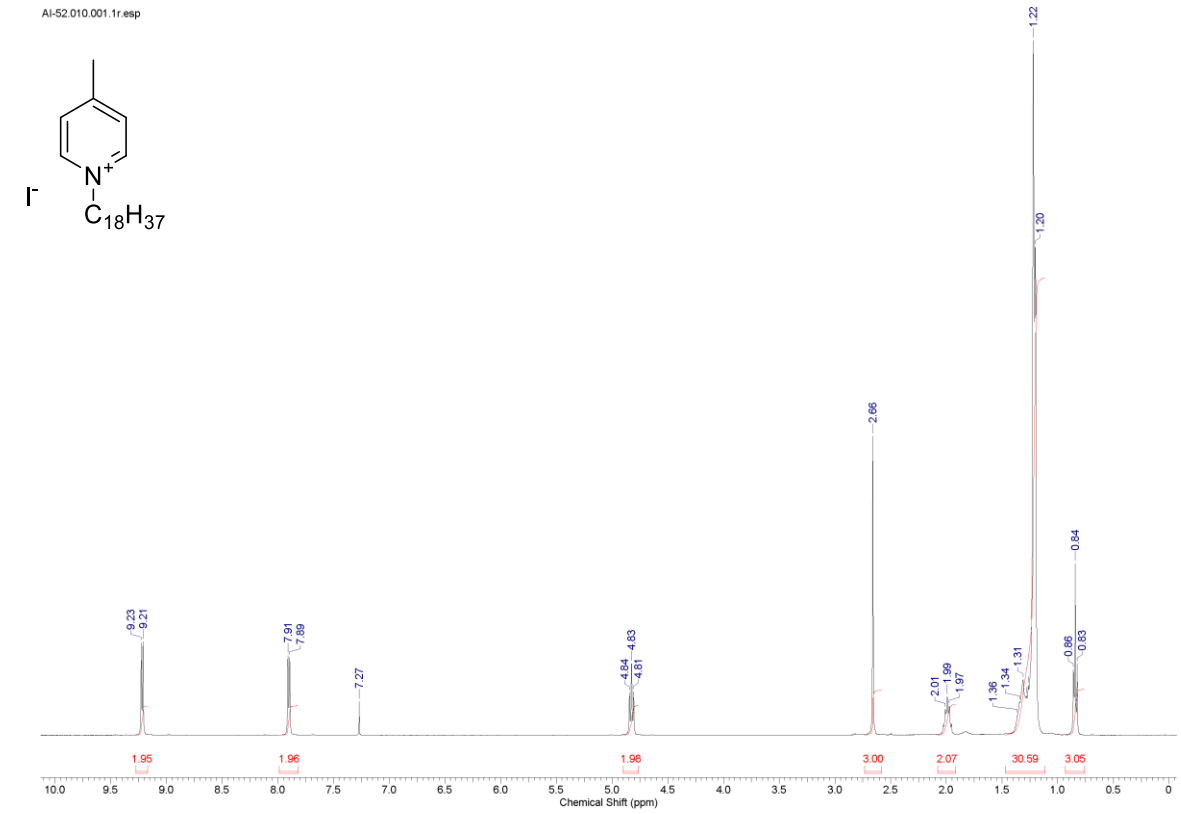

4-Methyl-1-octadecylpyridin-1-ium iodide **^{13}C NMR**:

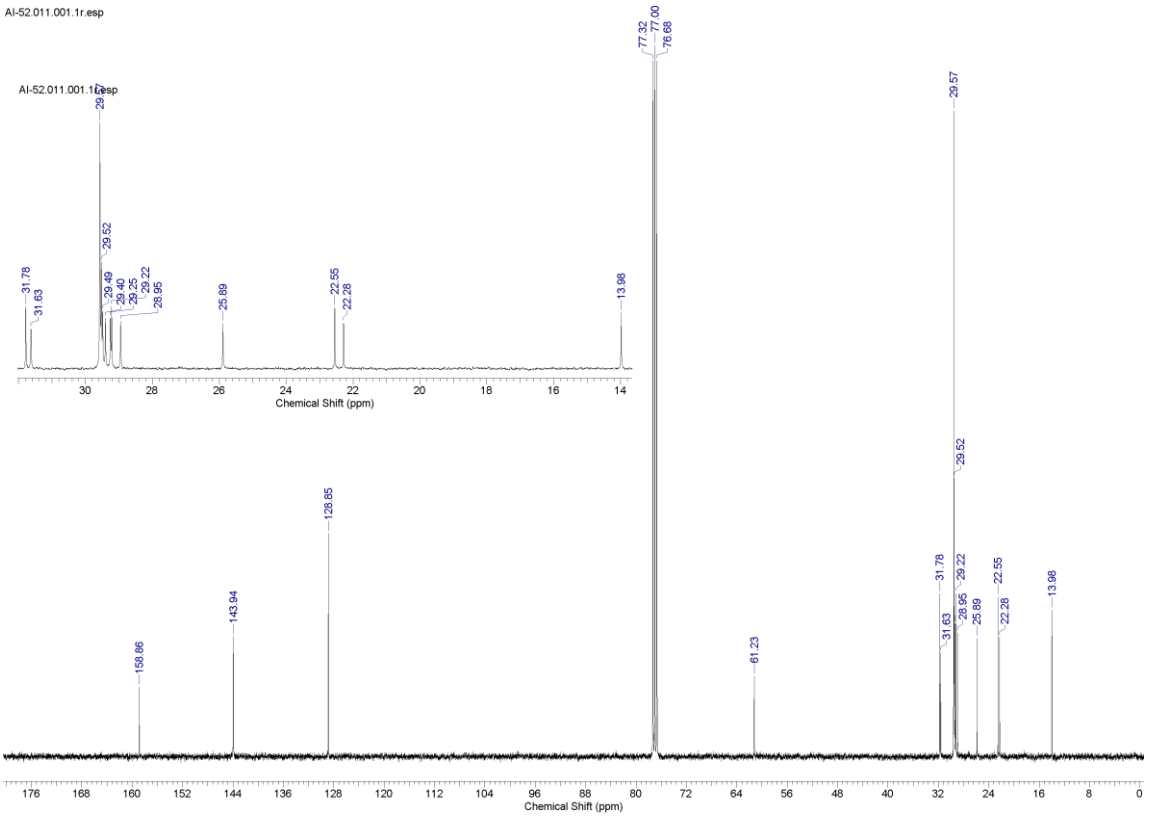

(*E*)-4-(4-(Diethylamino)styryl)-1-octadecylpyridin-1-ium iodide **^{1}H NMR**:

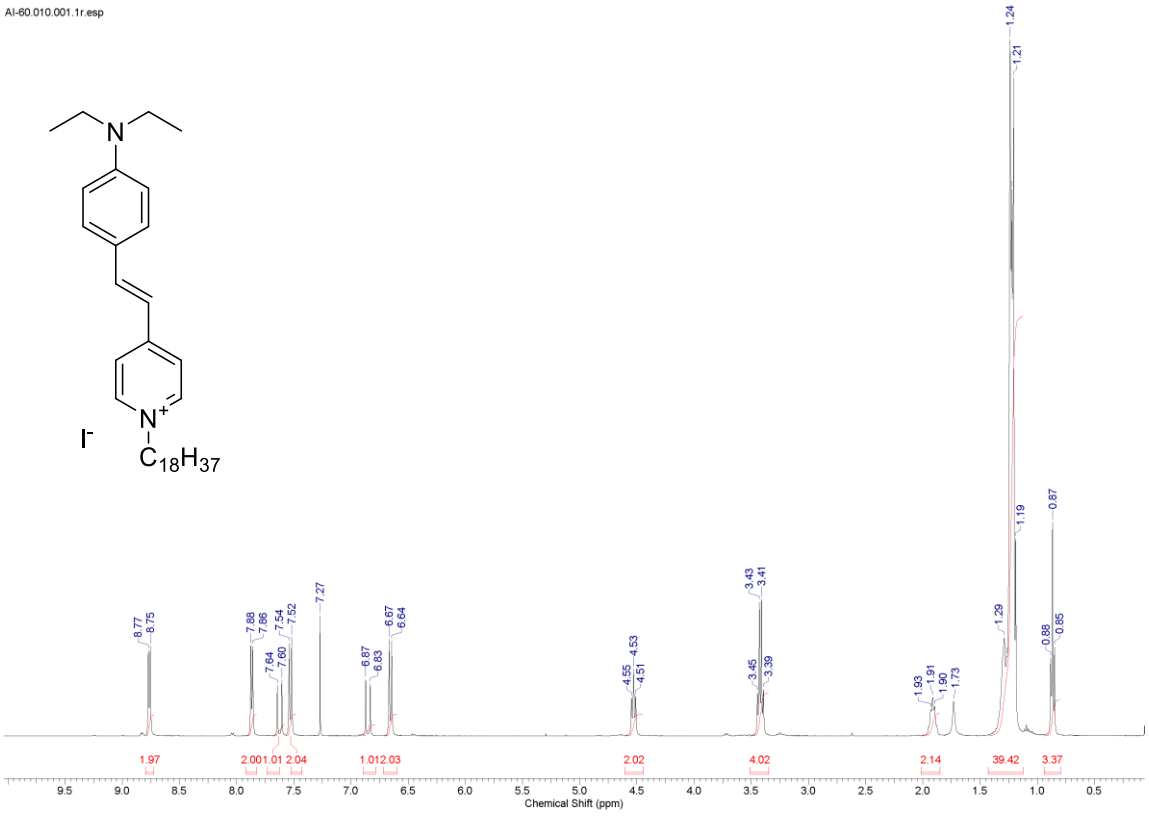

(*E*)-4-(4-(Diethylamino)styryl)-1-octadecylpyridin-1-ium iodide **^{13}C NMR**:

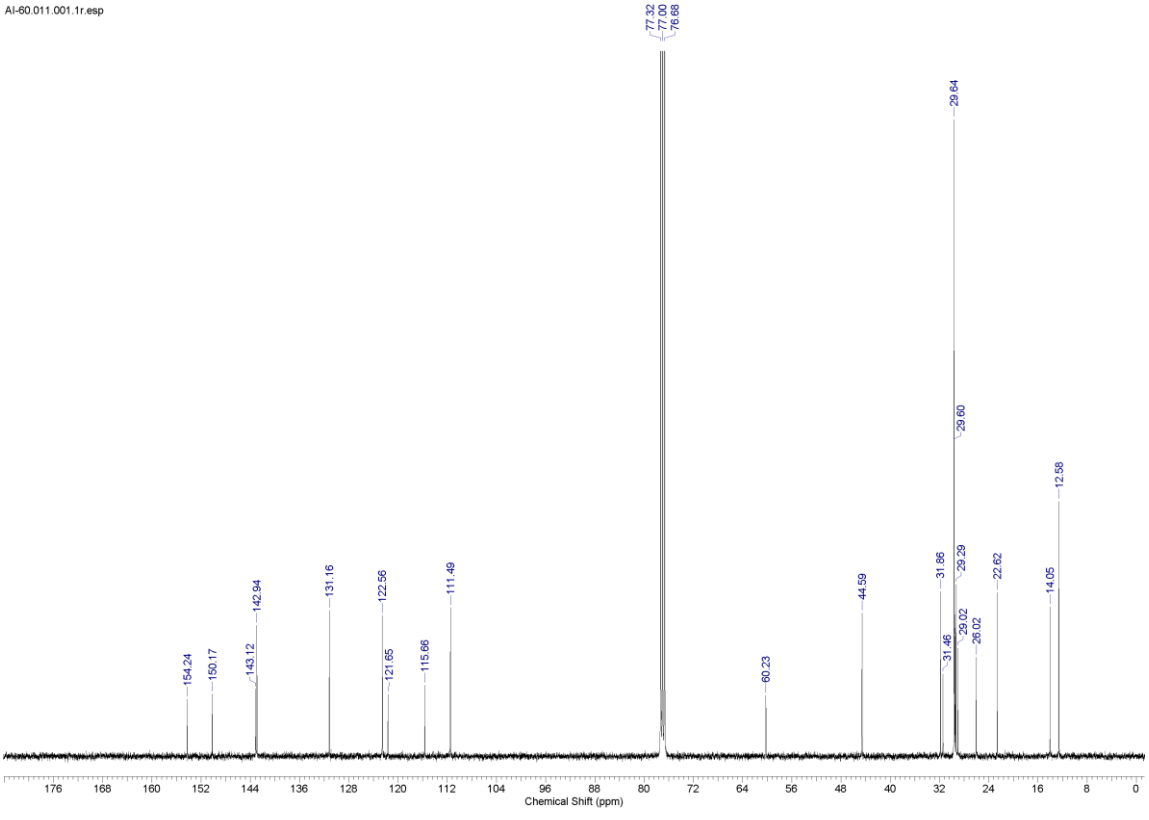

(*E*)-4-(4-(diphenylamino)styryl)-1-octadecylpyridin-1-ium iodide **^{1}H NMR:**

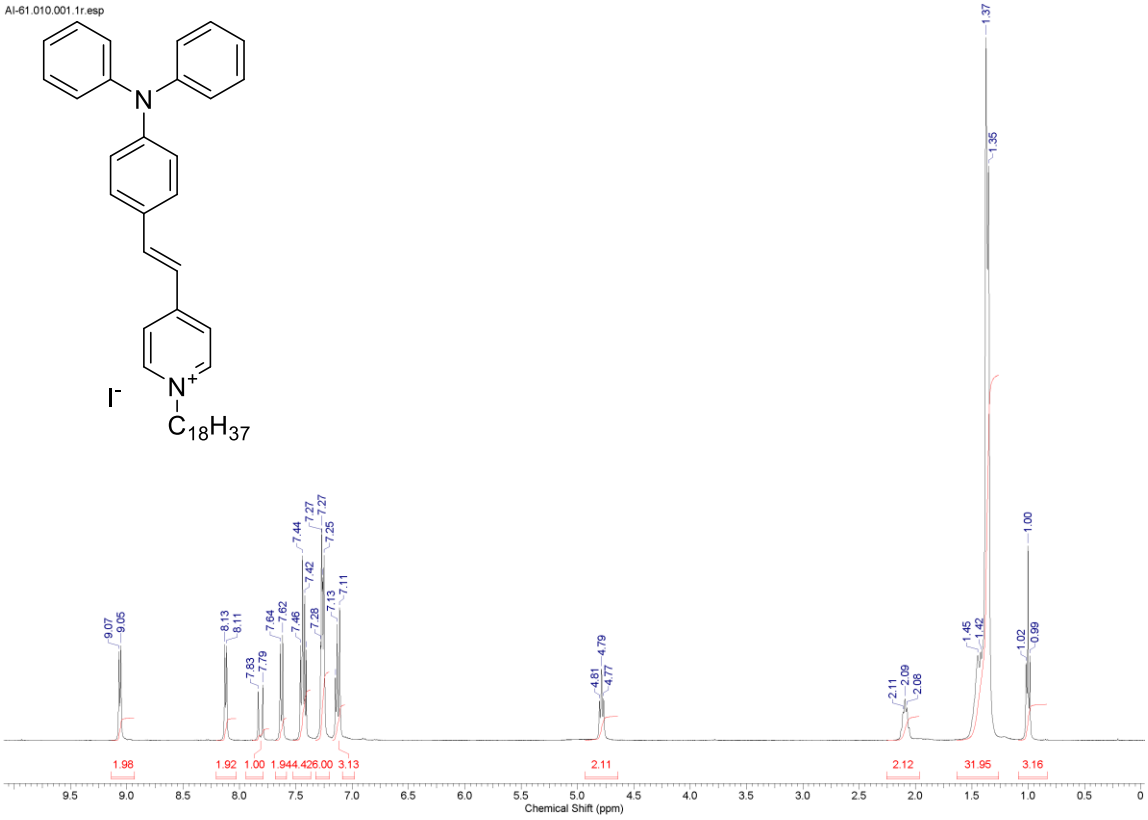

(*E*)-4-(4-(diphenylamino)styryl)-1-octadecylpyridin-1-ium iodide **^{13}C NMR**:

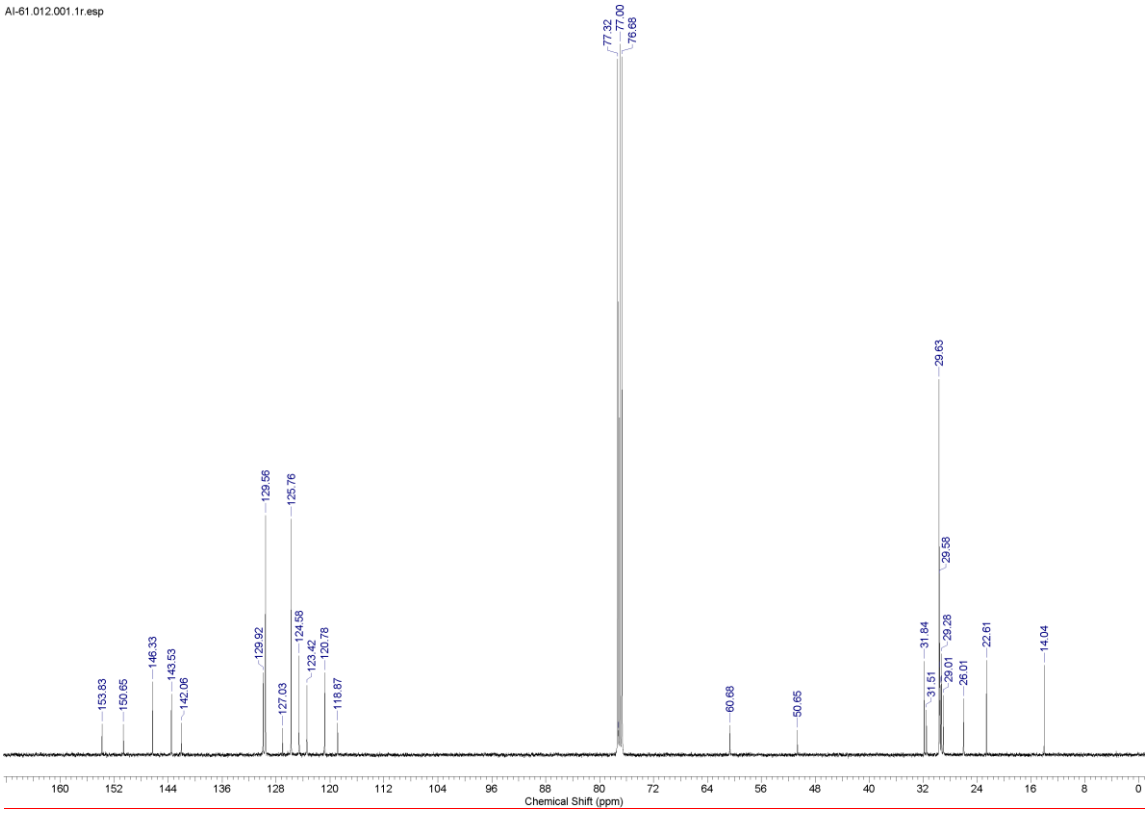

(*E*)-4-(4-(9H-Carbazol-9-yl)styryl)-1-octadecylpyridin-1-ium iodide **^{1}H NMR**:

(*E*)-4-(4-(9H-Carbazol-9-yl)styryl)-1-octadecylpyridin-1-ium iodide **^{13}C NMR**: